SEPARATION OF ISOTOPES VIA DYNAMICAL DELOCALIZATION

By

Sadam Hussain

DEPARTMENT OF ELECTRONICS
QUAID-I-AZAM UNIVERSITY
ISLAMABAD, PAKISTAN

January 2011

SEPARATION OF ISOTOPES VIA DYNAMICAL DELOCALIZATION

DISSERTATION

Thesis Submitted for the Partial Fulfillment of Requirement for Degree of

Master of Philosophy in Electronics

By

SADAM HUSSAIN

DEPARTMENT OF ELECTRONICS

QUAID-I-AZAM UNIVERSITY

ISLAMABAD, PAKISTAN

January 2011

CERTIFICATE

The undersigned hereby certify that they read and recommend to the Faculty of Graduate studies for the acceptance a thesis entitled ***"Separation of Isotopes Via Dynamical Delocalization"*** by **Sadam Hussain** in partial fulfillment of the requirements for the degree of **Master of Philosophy**

Dated: January 2011

Research Supervisor:

Dr. Farhan Saif
Associate Professor
Department of Electronics,
Quaid-i-Azam University, Islamabad, Pakistan.

Submitted Through:

Dr. Qaisar Abbas Naqvi
Associate Professor (Chairman)
Department of Electronics,
Quaid-i-Azam University, Islamabad, Pakistan.

DEDICATION

To the four pillars of my life: Allah, my brother, and my parents. Without you, my life would fall apart.

I might not know where the lifes road will take me, but walking with You,Allah, through this journey has given me strength.

Zahid, you are everything for me, without your love and understanding I would not be able to make it.

Mother, you have given me so much, thanks for your faith in me, and for teaching me that I should never surrender.

Father, you always told me to reach for the stars. I think I got my first one. Thanks for inspiring my love for transportation. We made it...

Acknowledgments

All praises and glories be to Allah, the Almighty and the Most Merciful, for the wonderful opportunities with which I have been blessed.Also peace be upon His beloved, the great Holy Prophet Hazrat Muhammad (S.A.W), who told us the way to gain wisdom and to bring positive revolution in the word. I hold the deeper respect for my university which provided me a chance, competitive environment and every facility which I needed for my research work. I owe my profound thanks to my supervisor, Dr. Farhan Saif for his keen interest, invaluable suggestions, inspiring attitude and encouragements throughout my research work. I feel proud to pay gratitudes to all of my teachers, especially to Dr. Qaiser Abbas Naqvi, Dr. Syed Aqeel Bukhari, Dr. Hassan Mehmood,Dr. Aqeel Ashraf, Arshad Hussain and Zeshan Akbar who imparted their knowledge and skills throughout my M.Sc. and M.Phil period for the grooming of my knowledge and thought and broaden my horizon in the field of Electronics.

These acknowledgements will remain incomplete without mentioning my family and friends. My especial gratitude is for my parents, their love and support has been with me throughout my educational career. I solute my father who is the real architect of my career. The dream of my late mother became true with the completion of this work. Her soul will be very happy because she is around us in our dreams, heart and all ours. Not forgettable is my brother(Dr Zahid Hussain) hours long discussions and technical support in my thesis.I am also thankful to my brother Khadim Hussain who give me the courage to get this award.

I thank to my seniors for their encouragement specially Jamil Hussain, Hayatullah and Mazhar Javed Khan for their kind support and guidance during my work,my colleagues Muhammad Asjad, Munir, Awais Haider and Abdul

for continuous help and valuable discussions through out my research work and my friends Zaibullah, Farmanullah, Atta u Rehman and Muhammad Umer.

Last but not least, truly on top of all, I and my thesis are immeasurably indebted to Muhammad Yameen Khan Jadoon himself.

Sadam Hussain

January 2011

Abstract

A method for the isotopes separation based on the dynamical de-localization phenomenon, that is purely Quantum phenomenon, is proposed. In this method we use the atomic Fermi accelerator. A particular value of modulation strength forces isotope of heavier masses, show diffusion and spread above the modulated atomic mirror while the other isotope of lighter masses show localization. Using an intense laser beam, we extract localized isotope and store in a chamber.

List of Figures

2.1 Snell's law 11

2.2 We see that for$\lambda = 0.8$ the Gaussian wave packet is exponentially Localized while for λ= 1.2 the width of Gaussian wave packet increases and it become Delocalized. 25

3.1 Experimental model 34

3.2 Triangular potential well 35

3.3 Autocorrelation function is plotted against scaled evolution time $\kappa = 4$. 40

3.4 Autocorrelation function plotted against scaled evolution time $\kappa = 1$. 41

3.5 The square of dispersion in momentum (ΔP^2) is plotted against modulation strength(λ) 42

3.6 The square of dispersion in momentumΔP^2 is plotted against modulation strengthλ for $\kappa = 4$ 43

3.7 This plot shows that in $(\lambda - \omega)$ space there are three regions:Region I where both of the Isotopes are Localized.Region II where Isotope for which $\kappa = 3$ correspond to large mass is delocalized and Isotope for which $\kappa = 4$ which correspond to small mass are localized.In region III both Isotopes are delocalized. 44

3.8 The square of dispersion in momentum (ΔP^2) is plotted against time for inside region.we find the smaller atoms localized and heaver mass delocalized. 45
3.9 The square of dispersion in momentum (ΔP^2) is plotted against modulation strength(λ) for Cesium atoms(Cs_{139}) 45
3.10 The square of dispersion in momentum (ΔP^2) is plotted against modulation strength(λ) for Cesium atoms(Cs_{132}) 46
3.11 This plot shows that in ($\lambda - \omega$) there are three regions.Region I where both of the Cesium(Cs) Isotopes are Localized.In region II Cs_{139} Isotope is delocalized and Cs_{132} are localized.In region III both Isotopes are delocalized.As we know location of localization region so by using intense laser beam we can collect Cs_{132} atoms in a chamber. 47
3.12 The square of dispersion in momentum (ΔP^2) is plotted against modulation strength(λ) for Hydrogen atoms(H_3)($Tritium$) . . 48
3.13 The square of dispersion in momentum (ΔP^2) is plotted against modulation strength(λ) for Hydrogen atoms(H_2)($Deuterium$) 48
3.14 This plot shows that in ($\lambda - \omega$) there are three regions.Region I where both of the Hydrogen(H) Isotopes are Localized.In region II H_3 Isotope is delocalized and H_2 are localized.In region III both Isotopes are delocalized.As we know location of localization region so by using intense laser beam we can collect H_2 atoms in a chamber. 49

Contents

1 Introduction **1**

1.1 Introduction 1

1.2 Types and representation of the isotopes 1

1.3 Isotope separation techniques 3

1.4 Layout 8

2 Atomic mirrors, Atomic traps and Dynamical localization **10**

2.1 Atomic mirror 10

2.2 Atomic traps 12

2.3 Dynamics of an atom in a laser field 13

2.3.1 Dipole radiation force 13

2.3.2 Radiation force in an evanescent laser wave field . . . 15

2.3.3 Radiation force in a standing laser wave 16

2.4 Optical atomic traps 17

2.4.1 Far-off-resonance dipole traps (FORT) 18

2.4.2 Quasi-electrostatic dipole traps (QUEST) 19

2.4.3 Trapping in standing laser waves 20

2.4.4 Trapping in optical waveguide modes 21

2.5 Atomic cavities 24

2.6 Dynamical localization 24

3 Isotope Separation Via Dynamical Delocalization **30**

3.1 Introduction 30

3.2 Dynamical localization of atoms in localization window 31

3.3 Principle of separation 33

3.4 Experimental model 34

3.5 System Hamiltonian 37

3.6 Numerical calculation 38

3.6.1 An analysis 39

3.7 Numerical results 40

4 Conclusions **50**

Chapter 1

Introduction

1.1 Introduction

Isotopes are atoms that contain the same number of protons but a different number of neutrons.Literally it means "equal place" and was formed from two Greek words, the prefix iso- "equal" and the noun topos "place". The reason for is that although isotopes of the same element have different atomic weights, they occupy the "same place" in the periodic table of elements.
Isotopes have the same Chemical properties due to the same number of electrons in their valence shell. Kinetic and thermodynamic properties of the element are also alter by mass difference. The physical properties of Isotopes are always different,but the nuclear properties of the Isotopes specifically have radioactive nature are widely different.

1.2 Types and representation of the isotopes

There are two types of Isotopes.
(i) Stable Isotopes (ii) Unstable (Radioactive) Isotopes

Stable isotopes are those which may or may not be radioactive, but if radioactive, have half lives too long to be measured. Isotopes that are classed as stable are predicted to have extremely long half-lives. If the predicted half-life falls into an experimentally accessible range, such isotopes have a chance to move from the list of stable nuclides to the radioactive region, once their activity is observed. Best examples are bismuth-209 and tungsten-180 which were formerly classed as stable, but have been recently (2003) found to be alpha-active. However, such nuclides do not change their status as primordial when they are found to be radioactive.

Unstable (Radioactive) Isotopes are those Radionuclide's that have been experimentally observed to decay, with half lives longer than 60 minutes are called Unstable Isotopes. Naturally occurring unstable isotopes (radionuclide's) fall into three categories (i) Primordial radionuclide's (ii) secondary radionuclide's and (iii) cosmogenic radionuclide's. Primordial radionuclide's originate mainly from the interiors of stars and, like uranium and thorium, are still present because their half-lives are so long that they have not yet completely decayed. Secondary radionuclides are radiogenic isotopes derived from the decay of primordial radionuclides. They have shorter half-lives than primordial radionuclides. Cosmogenic isotopes, such as carbon-14, are present because they are continually being formed in the atmosphere due to cosmic rays.

All elements having Isotopes are represented by their symbol putting the mass number as a left superscript e.g. $.^{235}U.^{238}U.^{239}U.$.In case of Hydrogen each of the Isotopes is represented by separate symbol and names.

1.3 Isotope separation techniques

Isotope separation is the process of concentrating specific isotope of a chemical element by removing other isotope of the same element, for example separating natural uranium into enriched uranium and depleted uranium.Isotopes are important due to their physical and nuclear properties. Some of the most important applications of the isotopes are given as following.

Radioisotope thermoelectric generator: A radioisotope thermoelectric generator (RTG, RITEG) is a nuclear electrical generator obtain its power from radioactive isotopes. In such a device, the heat released by the decay of a suitable radioactive material is converted into electricity by the Seebeck effect using an array of thermocouples.

Nuclear weapons: Uranium and plutonium are composed of several isotopes, some of which are used in fission process. These isotopes are used to produce an explosive devices for defence purposes.

Nuclear Medicine: This is a branch of medicine that uses radiation to provide information about the functioning of a person's specific organs or to treat disease. In most cases, the information is used by physicians to make a quick, accurate diagnosis of the patient's illness. The thyroid, bones, heart, liver and many other organs can be easily imaged, and disorders in their function revealed. In some cases radiation can be used to treat diseased organs, or tumours.

Agricultural Applications - radioactive tracers: Radioisotopes help to understand chemical and biological processes in plants. This can be done easily because (1) radioisotopes are chemically identical with other isotopes of the same element and will be substituted in chemical reactions and (2) radioactive forms of the element can be easily detected with a Geiger counter or

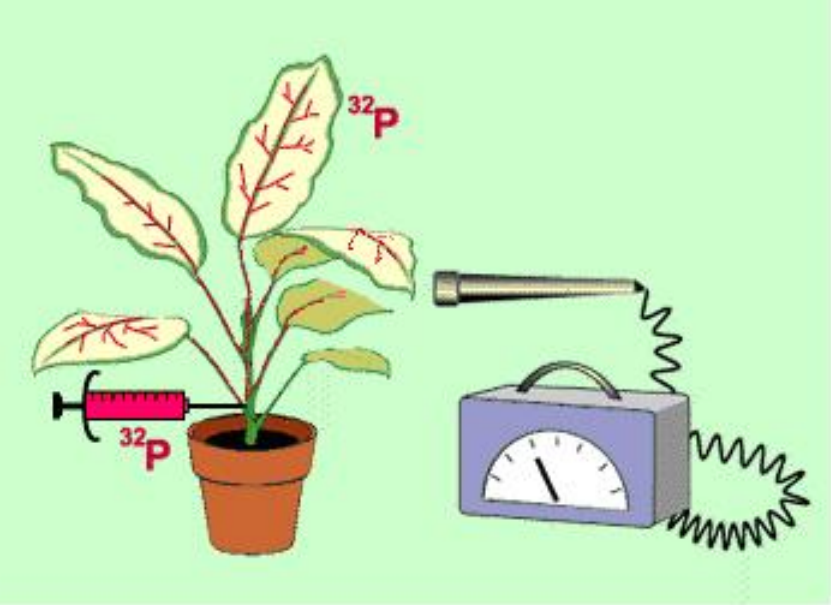

other such device.

Example:A solution of phosphate, containing radioactive phosphorus-32, is injected into the xleym of a plant. Experiment show that phosphorus-32 behaves identically to that of phosphorus-31, it is used by the plant in the same way. A Geiger counter is then used to detect the movement of the radioactive phosphorus-32 throughout the plant. This information helps scientists to understand the detailed mechanism of how plants utilized phosphorus to grow and reproduce.

Archaeological Dating: Significant progress have been made in the field of archaeology, due to the discovery of radioactivity and its properties. One application is carbon-14 dating. We know that all biologic organisms contain a given concentration of carbon-14, we can use these information to help

solve questions about when the organism died. When an organism dies it has a specific ratio by mass of carbon-14 to carbon-12 within the cells of its body. (The same ratio as in the atmosphere.) At the moment of death, no new carbon-14 containing molecules are generated; therefore the ratio is at a maximum. After death, the carbon-14 to carbon-12 ratio begins to decrease because carbon-14 is decaying away at a constant and predictable rate. Remembering that the half-life of carbon-14 is 5700 years,from this we find when the organism dies. **Separation techniques** There are three types of isotope separation techniques,

(i)Which are based on the atomic weight of the isotope,

(ii)The small differences in chemical reaction rates produced by different atomic weights,

(iii) Properties not directly connected to atomic weight,such as nuclear resonances.

Practical separation techniques all depend in some way on the atomic mass. It is therefore generally easier to separate isotopes with a larger relative mass difference. For example deuterium has twice the mass of ordinary (light) hydrogen and it is generally easier to purify it than to separate uranium-235 from the more common uranium-238.

Practical methods of separation:

(1) Diffusion: This method is based on the principle that in thermal equilibrium, two isotopes with the same energy will have different average velocities. The velocity of lighter atoms or molecules will be greater and be more likely to diffuse through a membrane. The difference in speeds is proportional to the square root of the mass ratio, so the amount of separation is small and many cascaded stages are needed to obtain high purity. This method is expensive due to the work needed to push gas through a membrane and the

many stages necessary.This technique is developed for gases, but also applicable for liquids.

(2) Centrifugal effect: In this scheme the material is rapidly rotated in a cylinder so the heavier isotopes go closer to an outer radial wall. This technic is often done in gaseous form using a Zippe-type centrifuge.

(3) Electromagnetic: This method is based on the deflection of charged particle in a magnetic field and the amount of deflection depends upon the particle's mass.This method is also known as mass spectrometry.It is very expensive method to produce large quantity, as it has an extremely low throughput, but it can allow very high purities to be achieved. This method is often used for processing small amounts of pure isotopes for research or specific use, but is impractical for industrial use.

(4) Laser Isotope separation: The interaction of the electromagnetic radiations with the atoms or molecules depends upon the mass difference. This results different hyperfine interactions. This can be used for the separation of the isotopes using laser. There are various methods for the separation of isotopes by the use of laser. Two of these are; i: Atomic vapour laser isotope separation (AVLIS) and ii: Molecular laser isotope separation (MLIS) **AVLIS** uses finely tuned laser for the ionization of a specific isotope. The tuned laser is absorbed only by particular isotope. The energy of the laser is enough for ionization. The ions produced by this interaction are easily separated by the use of an electric or magnetic field. In case of MLIS the composition of the gaseous molecules is changed on the basis of the mass of molecule. For example in uranium enrichment process, uranium is converted into uranium hexa-fluoride. When a beam of IR laser is shine on uranium hexa-fluoride it excites only U-235 containing UF_6. Another beam of laser converts the excited molecule into UF_5, which precipitates down from the

gaseous mixture.

(5) Chemical methods: Lighter isotopes tend to react or evaporate more quickly than heavy isotopes is the principle used in Chemical method .Lighter isotopes also disassociate more rapidly under an electric field. This method is most effective for lighter atoms such as hydrogen.This method is used to produced heavy water commercially.

(6) Wave packet isotope separation: The method of Wave packet laser isotope separation is based on long-time free evolution of wave packet. In this method we excite molecular or atomic wave packets through laser. The wave packet evolve in potential and due different masses evolution time is different for different isotopes. After some time revivals of wave packet occur and due to inharmonicity of the potential de-phasing of the wave packet occurs. so in this way we separate different masses from each others.

(7) Gravity: The gravity separation method is based on the mass difference of the isotopes.It is applicable to lighter elements such as oxygen and nitrogen.The gaseous compounds or the gaseous elements are cooled near their boiling point in very tall columns.The heavier isotopes go to the bottom and the lighter isotopes rise to surface, where they are easily collected. This process is also known as "cryogenic distillation", and was developed in the late 1960s by scientists at Los Alamos National Laboratory.

(8) Separation via dynamical localization: A new method to separate different isotopes of a material based on dynamical effects in modulated gravitational cavity.This method is based on purely Quantum phenomenon i.e. dynamical localization.In this method we use the atomic Fermi accelerator.For a particular value of modulation strength atoms of heavier masses show diffusion and spread above the modulated atomic mirror while atoms of lighter masses show dynamical localization. From our numerical calculation

we know position of localized atoms so by the use of intense laser beam we collect the localized atoms in a chamber.
Our method of separation is different from Diffusion,Centrifugal effect,Chemical method,Electromagnetic (Mass spectrometry) and Gravity because all these methods depend directly on mass difference and based on Classical principle while our method of separation based on Quantum phenomenon.It is also different from wave packet isotope separation because it is based on different evolution time of wave packet while in our method atoms are separated due to localization and delocalization regions.Similarly in laser isotope separation we use finely tune laser to ionize particular atoms but all of the atoms does not ionized so we can not get all of the particular atoms from the sample while in our method of separation we use radiation pressure of laser(electromagnetic wave) to collect localize atoms.

1.4 Layout

We thoroughly explain all these in the next chapters.
Atomic mirror
Atomic traps
Dynamics of an atom in a laser field
Optical atomic traps
Atomic cavities
Dynamical localization
Dynamical localization of atoms in localization window
Principle of separation via dynamical delocalization

Experimental model

System Hamiltonian

Numerical calculation

Numerical results

Chapter 2

Atomic mirrors, Atomic traps and Dynamical localization

2.1 Atomic mirror

Atomic mirror is a surface which exert exponentially increasing repulsive or attractive force on an approaching atom,as blue and red detunne [6] . An atomic mirror is obtained by an exponentially decaying optical field or an evanescent wave field [7].

To generate an evanescent wave field we consider an electro-magnetic field

$$\vec{E}(r,t) = \vec{E}(r)e^{-\iota\omega_f t} \tag{2.1}$$

which travels in a dielectric medium with a dielectric constant, n and undergoes total internal reflection. The electro-magnetic field inside the dielectric medium reads

$$\vec{E}(r,t) = E_0 e^{\iota\hat{k}r-\iota\omega_f t}\hat{e}_r \tag{2.2}$$

where, $\hat{e}_r$ is the polarization vector and $\hat{k} = k\hat{k}$ is the propagation vector. The electro-magnetic field,$\vec{E}(r,t)$, is incident on an interface between

the dielectric medium with the dielectric constant, n, and another dielectric medium with a smaller dielectric constant, n1. The angle of incidence of the field is θ_i with the normal to the interface. Since the index of refraction n1 is smaller than n, the angle θ_r at which the field refracts in the second medium, is larger than θ_i. As we increase the angle of incidence θ_i, we may reach a critical angle,$\theta_i = \theta_c$, for which $\theta_r = \frac{\Pi}{2}$. According to Snell's law, we define this critical angle of incidence as

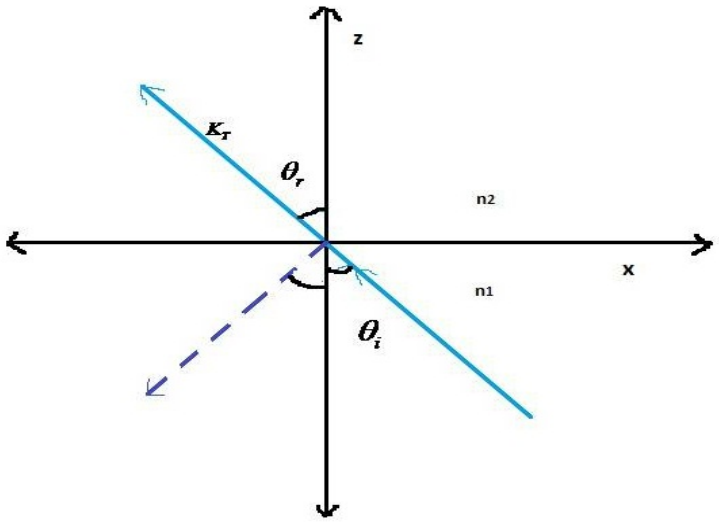

Figure 2.1: Snell's law

$$K_T = K_T \sin\theta_r \hat{x} + K_T \cos\theta_r \hat{z} \tag{2.3}$$

$$n_2 \sin\theta_r = n_1 \sin\theta_i \tag{2.4}$$

$$\theta_c \equiv \arcsin(\frac{n_1}{n_2}) \tag{2.5}$$

so $\cos\theta_r$ become complex. Hence, for an electro-magnetic wave with an angle of incidence larger than the critical angle, that is, $\theta_i > \theta_c$, we find the

inequality, $\sin\theta_r > 1$ [8]. As a result, we deduce that θ_r is imaginary, and define

$$\cos\theta_r = \iota\sqrt{(\frac{\sin\theta_i}{\sin\theta_c})^2 - 1} \tag{2.6}$$

Therefore, the field in the medium of smaller refractive index, n1, reads

$$\vec{E}(r,t) = \hat{e}_r E_0 e^{\iota k_1 \sin\theta_r + \iota k_1 z\cos\theta_r} e^{-\iota\omega_f t} = \hat{e}_r E_0 \hat{e}^{-kz} e^{\iota(\beta x - \omega_f t)} \tag{2.7}$$

where, $\kappa = k_1\sqrt{(\frac{\sin\theta_i}{\sin\theta_c})^2 - 1}$ and $\beta = k_1\frac{\sin\theta_i}{\sin\theta_c}$ [9].

Here, k1 defines the wave number in the medium with the refractive index n1. This demonstrates that in case of total internal reflection the field along the normal of the interface decays in the positive z-direction, in the medium with the smaller refractive index. In1987, Balykin and his coworkers achieved the first experimental realization of an atomic mirror [10]. They used an atomic beam of sodium atoms incident on a parallel face plate of fused quartz and observed the specular reflection. They showed that at small glancing angles, the atomic mirror has a reflection coefficient equal to unity. As the incident angle increases a larger number of atoms reaches the surface and undergoes diffusion. As a result the reflection coefficient decreases. The reflection of atoms bouncing perpendicular to the mirror is investigated in reference [11] and from a rough atomic mirror studied in reference [12].

2.2 Atomic traps

Methods of atomic trapping depend on the forces acting on atom arising from its interaction with laser field, magnetic field, combination of laser field and magnetic field or gravitational field. On the basis of these fields, atomic traps can be divided into four major classes: (1) Optical traps; (2) Magnetic traps; (3) Megneto-Optical traps; (4) Gravito-optical traps. The understanding of optical traps is based on the dynamics of atom in laser field .

2.3 Dynamics of an atom in a laser field

Now we discuss the forces acting on two level atom in optical field.

2.3.1 Dipole radiation force

As an atom interacts with electrio-magnetic field $E(r,t)$, atomic dynamics is controlled by the potential,

$$V = -\vec{d}.\vec{E}. \tag{2.8}$$

Where, d is induced dipole moment. The force acting on atom due to interaction between induced dipole moment and electric field, is given as

$$\vec{F} = \nabla(\langle\vec{d}.\rangle\vec{E}) \tag{2.9}$$

Induced dipole moment $\langle d\rangle$ for two level atom interacting with monochromatic linearly polarized laser field $\overrightarrow{E} = \hat{e}E_0(r)\cos(kr - \omega t)$ is given as

$$\langle d\rangle = \rho_{12}d_{21}\exp(i\omega_0 t) + \rho_{21}d_{12}\exp(-i\omega_0 t),$$

where, ω_0 is transition frequency associated to two level atom, ρ_{12}, ρ_{21} are the density matrix elements and d_{12} and d_{21} are dipole matrix elements. Using Rotating wave approximation dipole matrix elements are chosen real, $d_{12} = d_{21} = d$. Using this condition in the equation of motion of density matrix elements, we can write induced dipole moment as

$$\langle d\rangle = d\sigma_{12}\exp(ikz + i\omega t) + d\sigma_{21}\exp(ikz - i\omega t), \tag{2.10}$$

where, σ_{12} and σ_{21} are the off diagonal elements of the density matrix. Solution of the equation of motion of density matrix elements gives

$$\sigma_{12} = {\sigma_{21}}^* = -\frac{\Omega(r)(\delta - kv + i\gamma)}{\gamma^2 + 2\Omega^2(r) + (\delta - kv)^2}, \tag{2.11}$$

where, $\Omega(r) = dE_0(r)/2\hbar$ is the Rabi frequency, $\delta = \omega - \omega_0$ is the difference between field frequency and atomic transition frequency and determines detuning,v is projection of atomic velocity along wave vector and 2γ is the natural atomic transition width. Using Eq.(2.9), force on two level atom can be written as the sum of two forces, $F = F_{rp} + F_{gr}$, where, F_{rp} and F_{gr} stands for radiation pressure force and gradient force respectively, given as

$$F_{rp} = \hbar k\gamma \frac{G(r)}{1 + G(r) + (\delta - kv)^2/\gamma^2}, \tag{2.12}$$

$$F_{gr} = -\frac{1}{2}\hbar(\delta - kv)\frac{\nabla G(r)}{1 + G(r) + (\delta - kv)^2/\gamma^2}. \tag{2.13}$$

Here $G(r)$ is saturation parameter given by

$$G(r) = \frac{2\Omega^2(r)}{\gamma} = \frac{1}{2}(\frac{dE_0(r)}{\hbar\gamma})^2 = \frac{I(r)}{I_s}, \tag{2.14}$$

where, $I(r)$ is laser intensity at point r and I_s is saturation intensity. From Eq.(2.12) and (2.13) it is clear that direction of radiation pressure force F_{rp}, is same as the direction of field and it is independent of the detuning. While the the direction of gradient force F_{gr} is dependents on the sign of detuning. If δ is positive than the force on atom is repulsive and if it is negative the force is attractive. If velocity of an atom is very low i.e; $|v| \ll |\delta|/k$ then the gradient force depends only on the position of atom . Lowest approximation can be done by putting $v = 0$ in the above equation, under this condition and large detuning, potential of the gradient force can be approximated as

$$U_{gr}(r) = \frac{\hbar\Omega^2(r)}{\delta}. \tag{2.15}$$

It is clear that total potential for slow moving atoms is slightly greater than gradient potential because of the potential due to radiation force.

2.3.2 Radiation force in an evanescent laser wave field

Electric field of evanescent wave is given as

$$\overrightarrow{E} = \hat{e}E_0 e^{-\alpha y}\cos(ky - \omega t), \tag{2.16}$$

where, $\hat{e}$ is unit polarization vector and α^{-1} is penetration depth of evanescent field in the vacuum, which depends on incident angle of laser light and on the refractive index of the dielectric by the following relation $\alpha = k\sqrt{n^2\sin^2\theta - 1}$. Evanescent wave is produced when laser light is totally internally reflected from the vacuum dielectric interface. Saturation parameter for evanescent wave field for two level can be written as

$$G(r) = G_0 e^{-2\alpha z}, \tag{2.17}$$

where, $G_0 = \frac{1}{2}(dE_0/\hbar\gamma)^2$ is saturation parameter at the interface. Putting the value of G(r) in Eq.(2.12) and (2.13) we can find forces on atom given as

$$F_{rp} = \frac{\hbar k\gamma G_0 e^{-2\alpha z}}{1 + G_0 e^{-2\alpha z} + (\delta - kv_y)^2/\gamma^2}\ , \tag{2.18}$$

$$F_{gr} = \hbar\alpha(\delta - kv_y)\frac{G_0 e^{-2\alpha z}}{1 + G_0 e^{-2\alpha z} + (\delta - kv_y)^2/\gamma^2}\quad . \tag{2.19}$$

As it is clear from Eq.(2.19) for low atomic velocity along the interface $|v_y| \ll |\delta|/k$ and $\delta > 0$, atom is pushed towards the vacuum. Hence the blue detunned evanescent wave is used in the atomic mirrors. We use in our work evanescent wave trap based on gradient force. In case of blue detuning potential of the gradient force under condition $|\delta| \gg \gamma, \Omega_0$ is calculated as

$$U_{gr} = \frac{\hbar\Omega_0^2}{8}e^{-2\alpha z} \tag{2.20}$$

2.3.3 Radiation force in a standing laser wave

Now we discuss the dynamics of atom in the standing field, defined as

$$\overrightarrow{E} = 2\hat{e}E_0 \cos(kz)\cos(\omega t) \tag{2.21}$$

Naturally mathematical expression for the force on atom in standing wave, is given in terms of Fourier series. At not very high intensity of standing laser field Fourier series can be truncated to the first oscillating terms, such truncation gives the result [13] as

$$F = F_0 + F_{2s}\sin(2kz) + F_{2c}\cos(2kz)\ , \tag{2.22}$$

where

$$F_0 = \hbar k\gamma \frac{G(L_- - L_+)}{1 + G(L_- + L_+)} \tag{2.23}$$

$$F_{2s} = \hbar k\gamma \frac{(\delta - kv)L_- + (\delta + kv)L_+)}{1 + G(L_- + L_+)}\ , \tag{2.24}$$

$$F_{2c} = -F_0\ , \tag{2.25}$$

and

$$L_+ = \frac{\gamma^2}{\gamma^2 + (\delta + kv)^2}\ ,$$

$$L_- = \frac{\gamma^2}{\gamma^2 + (\delta - kv)^2}\ ,$$

are Lorentzian factors. Note that the magnitude of the radiation force Eq.(2.22) averaged over the spatial period in the first-order approximation in the saturation parameter is close to the difference of two radiation pressure forces of form Eq.(2.12) and Eq.(2.13)

$$F_0 \approx \hbar k\gamma G(L_- - L_+) \tag{2.26}$$

At the weak resonance the averaged radiation force has the meaning of radiation pressure force. For slow atomic motion, $v = 0$, radiation force from Eq.(2.22) reduces to periodic gradient force, give as

$$F = F_{gr} = 2\hbar k\delta \frac{G}{1 + 2G + \delta^2/\gamma^2} \sin(2kz) \tag{2.27}$$

where, $G = 2\Omega^2/\gamma^2$, $\Omega = dE_0/2\hbar$. Periodic potential is given as

$$U = U_0 \cos(2kz), \tag{2.28}$$

where,

$$U_0 = \frac{\hbar\delta G}{1 + 2G + \delta^2/\gamma}. \tag{2.29}$$

At saturation parameter$G \gg \frac{1}{2}(1 + \delta^2/\gamma^2)$ or equivalently Rabi frequency $\Omega \gg \frac{1}{2}\sqrt{\gamma^2 + \delta^2}$ potential depth close to its asymptotic value $U_0 = \hbar|\delta|$. From Eq.(2.24) It is clear that, for red detuning ($\delta < 0$) minima of potential in in the loops of standing wave. When expanded to a first-order in velocity, radiation force Eq.(2.22) includes in addition to the gradient force Eq.(2.27) also the radiation pressure force proportional to the atomic velocity

$$F = 2\hbar k\delta \frac{G}{1 + 2G + \delta^2/\gamma^2} \sin(2kz) + 8\hbar k^2 \frac{\delta}{\gamma} \frac{G \sin^2 kz}{(1 + 2G + \delta^2/\gamma^2)(1 + \delta^2/\gamma^2)}. \tag{2.30}$$

At red detuning second part of Eq.(2.30) becomes the friction force, with periodic reflection coefficient β given below

$$\beta = 16\omega_r \frac{\delta}{\gamma} \frac{G \sin^2 kz}{(1 + 2G + \delta^2/\gamma^2)(1 + \delta^2/\gamma^2)} \tag{2.31}$$

2.4 Optical atomic traps

Atomic traps in which laser beam is used to trap the atom are known as optical traps. We have seen in the previous section that dynamics of atom

in laser field is controlled by three forces: (1) Radiation pressure force; (2) Dipole gradient force; and (3) Momentum diffusion. So these forces can be used to accelerate, decelerate and trap the atoms. For slowly moving atom in a far-detuned laser field the optical excitation is low, as a result, the radiation pressure force originating from the absorption of the laser light and the heating caused by the momentum diffusion are small. The minima of the potential produced by the dipole gradient force in a far-detuned laser field can thus be used for optical trapping of atoms. The life time of atoms in the trap is limited by the heating due to the momentum diffusion. The properties of the optical dipole traps largely depend on the magnitude of the detuning. The heating rate due to the momentum diffusion may be very small at a very large detuning. The diffusive heating always introduces an upper limit on the lifetime of atoms in the dipole traps. On the bases of laser field frequency with respect to the transition frequency of two level atoms there are two types of optical traps: (1) Far-off-resonance dipole traps; (2) Quasi-electrostatic dipole traps.

2.4.1 Far-off-resonance dipole traps (FORT)

In this type of trap detuning is assumed to satisfy the condition $\delta \gg \gamma, \Omega$, under this condition the effect of radiation pressure force can be neglected compared to that of gradient force. Using Eq.(2.20), the potential well of the trap at red detuning is given as

$$U_{gr}(r) = -\hbar^2 \frac{\Omega^2(r)}{|\delta|}. \tag{2.32}$$

The lifetime of atoms in a single-beam FORT is typically defined by the heating due to the momentum diffusion and the background gas collisions. The characteristic time of an atom escape from the FORT caused by the

diffusive heating, can be estimated from the potential well depth U_0 and momentum diffusion coefficients as

$$\tau = \frac{2MU_0}{D(0)} = \frac{|\delta|}{\omega_r \gamma}, \tag{2.33}$$

where, $D(0)$ is the momentum diffusion coefficient, M is the atomic mass and ω_r is the recoil frequency for the atoms. It is clear from the above equation that the life time of the trap time is directly proportional to the amplitude of the detuning. The first FORT was used to trap the sodium atoms [14]. In which they used laser of 220 mW at the detuning 130 GHz . Due to small amount of detuning trap was in few milliseconds and potential depth was also very small. The improved trap of this type is given [15], in which rubidium atoms in the beam of a titanium-sapphire laser was traped for 0.2 s. In the FORT formed by the intersection of two beams of Nd:YAG lasers ($\lambda = 1.06\mu m$) the life time of sodium atoms in the trap was improved to few seconds given in [16]. The effect of polarization on the life time of atoms in the FORT was studied by [17]. The trapping of rubidium atoms in hollow blue-detuned laser beams was reported by [18]. A scheme to trap atoms in a blue-detuned FORT formed by a single laser beam and a holographic phase plate was demonstrated by [19]. At a detuning in a region 0.1-30 nm 105 Rb atoms were trapped for 0.3 s at temperature of 24 K and a density of $7.10^{11} cm^{-3}$.

2.4.2 Quasi-electrostatic dipole traps (QUEST)

In the QUEST, the detuning of the laser beam is comparable with the optical frequencies of an atom. The most important advantage of the QUEST is an extremely low diffusion-associated heating of atoms and accordingly long lifetime of atoms. In a most careful experimental investigation of the

QUEST an ensemble of Cs atoms was trapped in a 20 W CO2 laser beam focused into a spot with the waist radius 100 m. The depth of the potential well, was estimated to be 115 mK and the the lifetime of the atoms in the trap, 10 s, was found to be governed by the factors other than the diffusion-associated heating, such as collisions with residual gas molecules and three-particle recombination [20, 21] demonstrated an ultrastable CO2 laser trap that provided tight confinement of atoms with negligible optical scattering and minimal laser-noice-induced heating. By this technique 6Li atoms were stored in 0.4 mK deep well with a lifetime of 300 s consistent with a background pressure of 10-11 Torr. .

Note finally that basic distinction between the FORT and QUEST consists in the value of the diffusion heating. Since the population of the excited atomic state in the QUEST is extremely small, the diffusion-associated heating of atoms in the QUEST is much smaller than in the FORT.

2.4.3 Trapping in standing laser waves

Periodic potential acts on two level atom placed near-resonant standing laser wave. Atoms at very low temperature are trapped for a long time in the minima of the periodic potential. This type of trap is not stable because of heating due to momentum fluctuations. Friction produced by the radiation pressure force can stabilize the energy (temperature) of the atoms at a level substantially lower than the potential well depth. This mechanism does not work for the two level atoms as in that case friction coefficient goes to to zero in the locality of potential minima. In case of red detuning, in addition to the periodic potential there also develops a periodic friction force that decelerates the atoms and facilitates their localization. In other words, the periodic potentials produced by counter-propagating laser waves in their turn

produce periodic gratings of cold atoms. Such atomic gratings are called optical lattices. A direct experimental proof of the localization of cold atoms in the periodic minima of a standing laser wave potential was obtained by observing the channeling of cold sodium atoms in curved potential wells produced by a spherical standing laser wave [22, 23]. The deflection of slow atoms was observed to occur as a result of their channeling both at the nodes of the standing laser wave in the case of blue detuning and at the loops in the case of red detuning [24].

Another experimental proof of the localization of cold atoms at the minima of a periodic optical potential was obtained by recording the resonance fluorescence spectra of cesium atoms trapped in the optical potential, either three-dimensional [25] or one-dimensional [26], produced by counter-propagating laser waves of linear and orthogonal polarization. Various types of three-dimensional optical lattices, both periodic and quasi periodic, have been realized by [27, 28, 29, 30]. These lattices were used to study the properties of localized cold atoms at temperatures of the order of 10-100 μK

2.4.4 Trapping in optical waveguide modes

A cold atoms trap, whose one or two linear dimensions are very large, can be treated and used as a waveguide for the de Broglie atom waves. One of the first optical trap-atom waveguide schemes was the scheme of a flat atom waveguide containing two evanescent laser waves with red and blue detuning [31]. The basic idea of this type of atomic trap is that, a blue-detuned evanescent wave produces a repulsive potential, while the red-detuned wave, an attractive potential. As a result of these two forces potential minima is created at some distance from the surface, due to which the motion of atoms is controlled in the direction vertical to the interface. The penetration

depth of red-detuned evanescent wave into the vacuum is kept greater than the blue-detuned wave. Evanescent waves are created by the total internal reflection of field at the vacuum dielectric interface. The incident angle of the red detuned laser field is kept slighter greater than the critical angle $\theta_r > \sin^{-1}(1/n)$, where, n is the refractive index of the dielectric medium in which field is totally internally reflected. The incident angle of blue detuned laser filed should be much more than the critical angle $\theta_b \gg sin^{-1}(1/n)$ these condition on the incident angles are necessary for the required penetration depth. The above mentioned atom waveguide can be used for the propagation of cold atoms in a plane parallel to the dielectric-vacuum interface. Using the laser beams of Gaussian intensity profile, this atom waveguide can be transformed into a three-dimensional trap, in which atoms are bound in specific region [32].

Later on there were suggested other flat atom waveguide schemes based on the use of both an optical potential [33, 34] and a magnetic potential [35]. It should be emphasized that it would naturally be sensible to speak of atom waveguide only in the case of sufficiently cold atoms possessing the wave properties. For not very cold atoms moving like classical particles. The above schemes play the role of the devices for transporting atoms in the desired direction or serve as one or two-dimensional traps. The first atom waveguide scheme to be practically verified was that where the atoms moved inside the intensity maximum of the optical mode EH11 propagating inside a hollow optical waveguide [36]. Generally speaking, many axially symmetric electromagnetic modes can be excited in a hollow cylindrical dielectric waveguide [37]. When the internal radius a of the waveguide is small enough, the principal mode is EH11 and the radial distribution of the electric field of the

mode EH11 in the cylindrical coordinates, z, ρ and ϕ has the form,

$$\overrightarrow{E} = \frac{1}{2}\hat{e}E_0 J_0(\chi\rho)e^{i(\beta z-\omega t)} + c.c, \tag{2.34}$$

where, $\hat{e}$ unit polarization vector and ρ and β are the complex propagation constant. For large large blue detuning, attractive potential for the atoms is written as

$$U = -\frac{\hbar\Omega_0^2}{|\delta|}J_0^2(\chi\rho) \tag{2.35}$$

where, Ω_0 is the Rabi frequency for the field. The above scheme was experimentally implemented for rubidium atoms [38], in which glass hollow-core fiber 3 cm long and 40 m in internal diameter was used. The laser light was launched into the hollow region of the glass fiber. A beam of rubidium atoms propagated in the dipole potential whose depth corresponded to an effective atomic temperature of 70 mK. This magnitude of the potential allowed atoms with transverse velocities of up to 40 cm/s to be transported through the waveguide. A considerable disadvantage of the waveguide based on the intensity maximum of an optical waveguide mode is the diffusion-associated heating of the atoms. For this reason, much more attractive are atom waveguides wherein atoms propagate in optical waveguide modes having the minima near the axis [39, 40, 41, 42]. At present, there exist various methods to generate such modes. A discussion of these methods can be found in the review on atom waveguides [43]. Subwavelength-diameter optical fiber having both red and blue detuned laser field was used to trap the atoms outside the fiber [44]. Input light fields of circular polarization were used. local minima was created at certain distance from the fiber so atom trap was created in the form of circular ring around the fiber. If both input lights are linearly polarized than potential minima is created at at two points around the fiber. So in this case atoms can be trapped along two straight lines parallel to the fiber axis.

2.5 Atomic cavities

Based on the combination of atomic mirror various kinds of atomic cavities have been suggested.Some of which are:

(1) Two atomic mirror cavity: A system of two atomic mirrors placed at a distance with their exponentially decaying fields in front of each other form a cavity or resonator for the de Broglie waves. The atomic cavity is regarded as an analog of the Fabry Perot cavity for radiation fields [45].

(2) Ring cavity: By using more than two mirrors, other possible cavities can be developed as well. For example, a ring cavity for the matter waves can be obtained by combining three atomic mirrors

(3) An atomic gravitational cavity:It is a special arrangement. Here, atoms move under gravity towards an atomic mirror, made up of an evanescent wave [46]. The mirror is placed perpendicular to the gravitational field. Therefore, the atoms observe a normal incidence with the mirror and bounce back. They exhaust their kinetic energy, later, moving against the gravitational field [47] and return. As a consequence, the atoms undergo a bounded motion in this atomic trampoline or atomic gravitational cavity. Hence, the evanescent wave mirror together with the gravitational field constitutes a cavity for atoms.

2.6 Dynamical localization

Dynamical Localization mean Quantum wave packet maintain it width in the momentum and position space.We take a particle in Fermi accelerator. In absence of external modulation the motion of particle is regular with no chaos.However as we introduce external modulation and increase modulation strength from a specific value i.e $\lambda \equiv \frac{K_{cr}}{4} \simeq 0.24$ the bouncing particle is no more restricted in classical domain and start diffusion whereas the corre-

sponding quantum dynamics display localization due to quantum interference phenomenon. A quantum particle,due to it non-locality, always experiences the modulation of the atomic mirror during its evolution in the Fermi accelerator. However, the classical counterpart feels the modulation of the mirror only when it bounces off.

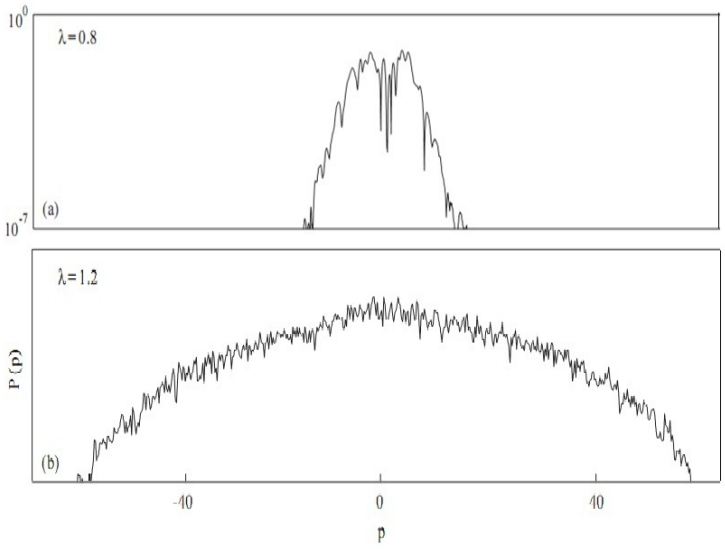

Figure 2.2: We see that for$\lambda = 0.8$ the Gaussian wave packet is exponentially Localized while for λ= 1.2 the width of Gaussian wave packet increases and it become Delocalized.

Here we also connect Anderson localization with dynamical localization.Anderson localization occurs in Configuration space while Dynamical localization happen in momentum and position space.

In1958, P.W. Anderson showed the absence of diffusion in certain random lattices[48] and gave birth to the phenomenon of Localization in solid-state physics-appropriately named as Anderson localization[49]. An electron, on a one-dimensional crystal lattice displays localization if the equally spaced lattice sites are taken as random. The randomness may arise due to the pres-

ence of impurities in the crystal. Thus, at each ith site of the lattice, there acts a random poterntial, T_i . The probability amplitude of the hopping electron, u_i , is therefore expressed by the Schrdinger equation

$$T_i u_i + \sum_{r=0} W_r u_{i+r} = E u_i \tag{2.36}$$

where W_r is the hopping amplitude from ith site to its rth neighbor. If the potential, T_i , is periodic along the lattice, the solution of the above eqn. is Bloch function, and the energy eigen values form a sequence of continuum bands. However, in case T_i are uncorrelated from site to site, and distributed following a distribution function, eigen values of the above eqn. are exponentially localized. Thus, in this situation the hopping electron finds itself localized. Twenty years later, Giulio Casati and coworkers suggested the presence of a similar phenomenon occurring in the kicked rotor model[50]. In their seminal work they predicted that a quantum particle, subject to periodic kicks of varying strengths, exhibits the suppression of classical diffusion.The phenomenon was named as *dynamical localization.* Later, on mathematical grounds,[51] developed equivalence between dynamical localization and the Anderson localization.

Dynamical Localization:-

$$\iota \frac{\partial}{\partial t} |\psi(t)\rangle = (H_0 + V\delta_T(t))|\psi(t)\rangle \tag{2.37}$$

1: Just before the Nth kick to (N+1)th kick.

$$|\psi(N+1)\rangle_- = e^{-\iota H_0} e^{-\iota V} |\psi(N)\rangle_- \tag{2.38}$$

Where $|\psi(N)\rangle_-$ describe the state of the system just before the Nth kick.

Let us now assume that one possible solution comes from the Floquet state that is

$$|\psi(N)\rangle_- = e^{\iota\omega_\alpha N} |U_\alpha(N)\rangle_- \tag{2.39}$$

and

$$|U_\alpha(N+1)\rangle_- = |U_\alpha(N)\rangle_- \tag{2.40}$$

Substituting in equ.(1) yields

$$|U_\alpha(N)\rangle_- = e^{-\iota(H_0 \mp \omega_\alpha)} e^{-\iota V} |U_\alpha(N)\rangle_- \tag{2.41}$$

Now introducing

$$e^{-\iota(H_0-\omega_\alpha)} = \frac{1-\iota T_\alpha}{1+\iota T_\alpha} \tag{2.42}$$

$$e^{-\iota V} = \frac{1-\iota W_\alpha}{1+\iota W_\alpha} \tag{2.43}$$

where

$T_\alpha = \tan[\frac{1}{2}(H_0^\wedge - \omega_\alpha)] = \tan[(\frac{1}{2}V)]$

leads us to

$$U_\alpha(N)\rangle_- = e^{-\iota(H_0 \mp \omega_\alpha)} e^{-\iota V} |U_\alpha(N)\rangle_-| = (\frac{1-\iota T_\alpha}{1+\iota T_\alpha})(\frac{1-\iota\omega_\alpha}{1+\iota\omega_\alpha})|U_\alpha(N)\rangle_- \tag{2.44}$$

$$[(1-\iota T_\alpha)(1-\iota\omega_\alpha) - (1+\iota T_\alpha)(1+\iota\omega_\alpha)]|U_\alpha(N)\rangle_- = 0 \tag{2.45}$$

$$\Rightarrow [(-\iota T_\alpha - \iota\omega) - (\iota T_\alpha + \iota\omega)]|U_\alpha(N)\rangle_- = 0 \tag{2.46}$$

$$\Rightarrow (T_\alpha + \omega)|U_\alpha(N)\rangle_- = 0 \tag{2.47}$$

$$\langle n|(T_\alpha + \omega)|U_\alpha(N)\rangle_- = 0 \tag{2.48}$$

Introducing the unit operator

$$\Sigma_m |n\rangle\langle n| = 1 \tag{2.49}$$

$$\sum_m \langle n|(T_\alpha|m\rangle\langle m| + W|m\rangle\langle m|)|U_\alpha\rangle_- = 0 \tag{2.50}$$

$$\sum_m \langle n|T_\alpha|m\rangle\langle m|U_\alpha(N)\rangle + \sum_m \langle n|W|m\rangle\langle m|U_\alpha(N)\rangle = 0 \tag{2.51}$$

$$\langle n|T_\alpha|m\rangle \ = \langle n|\tan[\frac{1}{2(H_0^\wedge - \omega_\alpha)}]|m\rangle = \tan(\frac{1}{4I}n^2 - \omega_\alpha)\delta_{nm} \tag{2.52}$$

$$T_\alpha(n)U_\alpha(n) + \Sigma_m\langle n|W|m\rangle U_\alpha(n) = 0 \tag{2.53}$$

$$T_\alpha(n)U_\alpha(n) + \Sigma_m W_{n,m}U_\alpha(n) = 0 \tag{2.54}$$

$$U_\alpha(n) = \langle n|U_\alpha(N)\rangle \tag{2.55}$$

$|n\rangle$ = Angular momentum states.

Hence we have written the equation for the Floquet states of the delta-kicked rotor in terms of a one dimensional tight binding model.The tight binding model describes the motion of an electron on a one dimensional lattice.

Therefore this approach connects a dynamical system with solid state physics problem.Here the angular momentum of the rotor corresponds to the lattice site in the solid state problem. Since

$$e^{-2\iota V} = \frac{\cos V - \iota \sin V}{\cos V + \iota \sin V} = \frac{1 - \iota \tan V}{1 + \iota \tan V} \tag{2.56}$$

T_n correspond to random potential in Anderson model , uncorrelated from site to site and distributed with density $\delta(T_m)$ [If$\delta(T_m)$ obeys Lagrangian distribution we have Lioyd's model]

If the potential T_n were periodic such that $T_{n+m} = T_n$ the solution of the Anderson equation is Bloch function and the energy eigen values would form a sequence of continuous bands.The occurrence of dynamical localization is attributed to the change in statistical properties of the spectrum[52]. The basic idea involved is that, integrability corresponds to Poisson statistics[53] however, non-integrability corresponds to Gaussian orthogonal ensemble (GOE) statistics as a consequence of the Wigner's level repulsion. In the Fermi-Ulam accelerator model, for example, the quasi-energy spectrum of the Floquet operator displays such a transition. It changes from Poisson statistics to GOE statistics as the effective Planck's constant changes in value[54] The study of the spectrum leads to another interesting understanding of localization phenomenon. Under the influence of external periodic force, as the system exhibits dynamical localization the spectrum changes to a pure point spectrum [55]. There occurs a phase transition to a quasi-continuum spectrum leading to quantum delocalization[56] for example, in the Fermi accelerator.

Chapter 3

Isotope Separation Via Dynamical Delocalization

3.1 Introduction

We investigate the quantum characteristics of an atom in Fermi accelerator which passes through amplitude modulated standing light wave. We consider two domain for our system, Classical domain and Quantum domain. For particular modulation strength the classical evolution in the system exhibits chaos and the atom display diffusion. However, in the quantum domain, the momentum distribution of the atom at the exit is exponentially or dynamically localized. As we increase modulation strength form an other critical value a phase transition occurs and the quasi-energy spectrum of the Floquet operator changes from a point spectrum to a continuum spectrum.
Hence, the two conditions together make a window on the modulation strength.

$$\lambda_l < \lambda < \lambda_c \tag{3.1}$$

Within the window classical diffusion sets in whereas the corresponding quantum dynamics displays localization. For the reason, we name it as localization window.

3.2 Dynamical localization of atoms in localization window

From the Analytical study of the atomic dynamics, we know that the dynamical localization occurs within a window of modulation strength, i.e.

$$\lambda_l < \lambda < \lambda_c \tag{3.2}$$

where $\lambda_l = \frac{K_{cr}}{4} = 0.24$ comes from Chirikov mapping[57] and describe the onset of classical diffusion.We express the classical dynamics of a particle in the Fermi accelerator by means of a mapping. The mapping connects the momentum of the bouncing particle and its phase just before a bounce to the momentum and phase just before the previous bounce. This way the continuous dynamics of a particle in the Fermi accelerator is expressed as discrete time dynamics. In order to write the mapping, we consider that the modulating surface undergoes periodic oscillations following sinusoidal law. Hence, the position of the surface at any time is $z = \lambda \sin t$, where λ defines the modulation amplitude. In the scaled units the time of impact, t is equivalent to the phase φ.

Furthermore, we consider that the energy and the momentum remain conserved before and after a bounce and the impact is elastic. As a result, the bouncing particle gains twice the momentum of the modulated surface, that is, $2\lambda \cos \varphi$, at the impact. Here, we consider the momentum of the bouncing particle much smaller than that of the oscillating surface.Moreover, it under-

goes an instantaneous bounce.

Keeping these considerations in view,we express the momentum, p_{i+1}, and the phase, φ_{i+1}, just before the $(i+1)$th bounce in terms of momentum, p_i, and the phase, φ_i, just before the ith bounce, as

$$p_{i+1} = -p_i - \Delta\varphi_i + 2\lambda \cos\varphi_i \tag{3.3}$$

$$\varphi_{i+1} = \varphi_i + \Delta\varphi_i \tag{3.4}$$

Here, the phase change $\Delta\varphi_i$ equivalent to the time interval, $\Delta t_i = t_{i+1} - t_i$, which defines the time of flight between two consecutive bounces. Hence, the knowledge of the momentum and the phase at the ith bounce leads to the phase change $\Delta\varphi_i$ as the roots of the equation,

$$p_i\Delta\varphi_i - \frac{1}{2}\Delta\varphi_i^2 = \lambda(\sin(\varphi_i + \Delta\varphi_i) - \sin\varphi_i) \tag{3.5}$$

We consider that the amplitude of the bouncing particle is large enough compared to the amplitude of the external modulation, therefore, we find no kick-to-kick correlation. Thus, we may assume that the momentum of the particle just before a bounce is equal to its momentum just after the previous bounce. The assumptions permit us to take,$\Delta\varphi_i \sim -2p_{i+1}$. As a result the mapping reads

$$p_{i+1} = p_i - 2\lambda \cos\varphi_i \tag{3.6}$$

$$\varphi_{i+1} = \varphi_i - 2p_{i+1} \tag{3.7}$$

We redefine the momentum as $P_i = 2p_i$, and $K = 4\lambda$. The substitutions translate the mapping to the standard ChirikovTaylor mapping, that is,

$$P_{i+1} = P_i + K \cos\varphi_i \tag{3.8}$$

$$\varphi_{i+1} = \varphi_i + P_{i+1} \tag{3.9}$$

Hence, we can consider the Fermi accelerator as a discrete dynamical system.The advantage of the mapping is that it depends only on the kick strength or chaos parameter, $K = 4\lambda$. Therefore, simply by changing the value of the parameter, K, the dynamical system changes from, stable with bounded motion to chaotic with unbounded or diffusive dynamics.
Upper limit $\lambda_c = \sqrt{\frac{\kappa}{2}}$ of the localization window describes the phase transition of the quasi-energy from point spectrum to a continuum spectrum. Above this limit quantum diffusion sets and destroy quantum localization and we find find quantum delocalization[58].

3.3 Principle of separation

This method is based on the principle of mass difference.From the concept of Localization window we know that the dynamical localization occurs within a window of modulation strength, i.e.

$$\lambda_l < \lambda < \lambda_c \tag{3.10}$$

where $\lambda_l = \frac{K_{cr}}{4} = 0.24$ comes from Chirikov mapping and describe the onset of classical diffusion and upper limit$\lambda_c = \sqrt{\frac{\kappa}{2}}$ of the localization window describes the phase transition of the quasi-energy from point spectrum to a continuum spectrum. Above this limit quantum diffusion sets and destroy quantum localization and we find find quantum delocalization. For two different isotopes of mass m1 and $m_2 = m_1 + \Delta m$, two different critical modulation strengths occur, i.e.$\lambda = \lambda_c^1$ for atoms of mass m_1 and $\lambda = \lambda_c^2$ for atoms of mass m_2.So we can easily find the localization region for particular Isotopes and separate it from other Isotopes through intense laser beam.

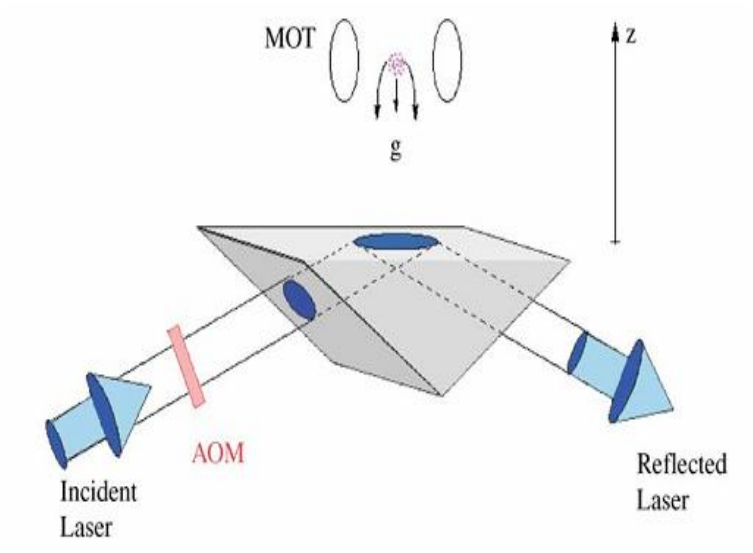

Figure 3.1: Experimental model

3.4 Experimental model

The model of our experiment is quite straight forward .We have a cloud of cooled atoms and trapped above the surface of a prism .

On the surface of Prism we have an evanescent wave field obtained by the total internal reflection of a laser light field .This evanescent wave field provides an exponentially rising force to the incoming atoms and therefore acts like a mirror for the atoms.

On joining an acusto-optic-modulator with the laser light field it is possible to provide a modulation to the evanescent wave field , which makes the system explicitly time dependent. $I_{(\tilde{z})}$ to $I_{(\tilde{z},\tilde{t})}$, i.e.

$$I_{\tilde{z},\tilde{t}} = I_0 \exp(-2k\tilde{z} + \epsilon \sin \omega t) \tag{3.11}$$

Fig. . (left) As we switch off the magneto-optic trap (MOT) at time, t = 0, the atomic wave packet starts its motion from an initial height. It

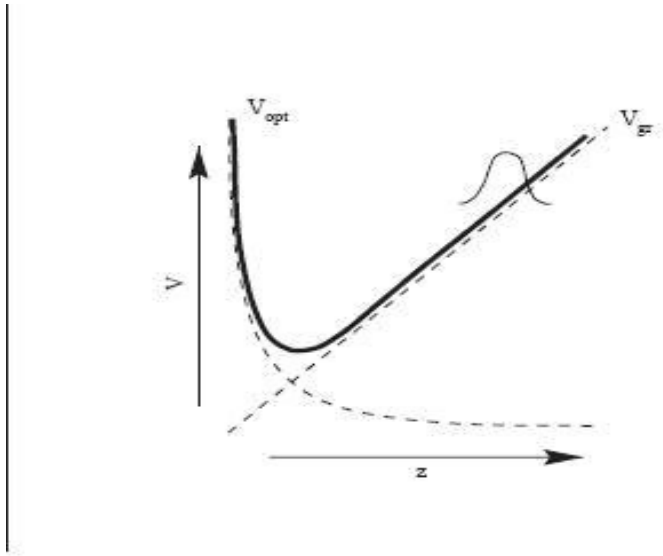

Figure 3.2: Triangular potential well

moves under the influence of the linear gravitational potential Vgr (dashed line) towards the evanescent wave atomic mirror. Close to the surface of the mirror the effect of the evanescent light field is dominant and the atom experiences an exponential repulsive optical potential Vopt (dashed line). Between the linear gradational potential and exponential potential the cloud of atoms observe a bounded motion.

Between the linear gravitational potential and exponential potential the cloud of atoms observe a bounded motion.

we may express the evanescent wave potential in z direction as

$$V = V_0 e^{\iota\kappa z} = V_0 e^{-kz} \tag{3.12}$$

$k = \iota\kappa$

Therefore the force exerted by exponential field on the atoms is

$$F_{opt} = -\nabla V = kV_0 e^{-kz} \tag{3.13}$$

For z large the atoms do not see the optical field and move under the

effect of gravitational field .On coming closer to the surface of the prism the atoms being highly detunned from the optical frequency experience a force F_{opt} the gravitational force is

$$F_g = -\nabla(mgz) = -mg \tag{3.14}$$

The quantity

$$V_0 = \frac{\hbar\Omega_e}{4}H = \frac{\hbar\Omega^2}{4\delta} = \frac{(\mu\varepsilon_0)^2}{4\delta\hbar} \tag{3.15}$$

And therefore depends inversely on the detunning δ. The atom moving with a velocity v bounces back when it kinetic energy exhausted against the height of the potential

$$\frac{\hbar\Omega_{max}^2}{4\delta} = \frac{1}{2}mv^2 \tag{3.16}$$

From here we can calculate the Ω_{max} required to reflect the atoms ,

$$\Omega = (\frac{2mv^2}{\hbar}\delta)^{\frac{1}{2}} \tag{3.17}$$

Probability of spontaneous emission is

$$P_{sp} = \gamma\frac{\Omega^2}{4\delta^2}\tau \tag{3.18}$$

where τ is the time spent in the optical field $\tau = \frac{1}{vk}$

Hence if δ is large the probability of spontaneous emission is less but a larger detunnig reduces the height of the potential ($\frac{\hbar\Omega^2}{4\delta}$). Therefore with increasing detunning δ we need to choose also larger intensity to keep the height of the potential constant. However this way we also inverse the probability of spontaneous emission.

Difference of $V_0(\alpha\frac{1}{\delta})$ and $P_{sp}(\alpha\frac{1}{\delta^2})$ provides a possibility to choose δ in such a way that P_{sp} is small enough and V_0 is also not small for a fixed Ω.

3.5 System Hamiltonian

The dynamics of the center-of-mass motion of the atoms in ground state follows from the Hamiltonian

$$\tilde{H} = \frac{\tilde{p^2}}{2m} + mg\tilde{z} + \frac{\hbar\Omega_{eff}}{4}e^{-2k\tilde{z}+\varepsilon\sin\omega\tilde{t}} \tag{3.19}$$

To simplify our numerical calculation, we make the variables dimensionless by introducing the scaling,$z \equiv \frac{\tilde{z}\omega^2}{g}$,

$p \equiv \frac{\tilde{p}\omega}{mg}$, $t \equiv \omega\tilde{t}$

put $\tilde{p} = \frac{pmg}{\omega}$, $\tilde{z} = \frac{zg}{\omega^2}$, $\tilde{t} = \frac{t}{\omega}$ in *equation*3.19 we get

$\tilde{H} = \frac{p^2mg^2}{2\omega^2} + \frac{zmg^2}{\omega^2} + \frac{\hbar\Omega_{eff}}{4}e^{-2\frac{kzg}{\omega^2}+\epsilon\sin t}$

dividing both sides by $\frac{mg^2}{\omega^2}$ we get the dimensionless Hamiltonian as

$$H \equiv \frac{p^2}{2} + z + V_o exp(-\eta(z - \varepsilon\sin t)) \tag{3.20}$$

Where dimensionless intensity $V_o \equiv \frac{\hbar\omega^2\Omega_{eff}}{4mg^2}$,

Steepness (*decaylength*) $\eta \equiv \frac{2kg}{\omega^2}$,

Modulation amplitude of the evanescent wave $\epsilon \equiv \frac{\omega^2\varepsilon}{2kg}$,

The commutation relation $[z, p] = \frac{[\tilde{z},\tilde{p}]\omega^3}{mg^2} = \frac{\iota\hbar\omega^3}{mg^2}$

Dimensionless plank's constant $\kappa \equiv \frac{\hbar\omega^3}{mg^2}$

3.6 Numerical calculation

Numerically we have the relation

$$\lambda_c = \frac{\sqrt{\kappa}}{2} \tag{3.21}$$

where $\kappa = \frac{\hbar\omega^3}{mg^2}$,

$$\kappa_1 = \frac{\hbar\omega^3}{m_1 g^2} \tag{3.22}$$

$$\kappa_2 = \frac{\hbar\omega^3}{m_2 g^2} = \frac{\hbar\omega^3}{m_1 g^2 + \Delta m g} \tag{3.23}$$

$$\lambda_c^{(1)} = \frac{\sqrt{\kappa_1}}{2} \tag{3.24}$$

$$\lambda_c^{(2)} = \frac{\sqrt{\kappa_2}}{2} = \frac{1}{2}\sqrt{\frac{\hbar\omega^3}{(m_{1+\Delta m})g}} \tag{3.25}$$

$$\lambda_c^{(2)} = \frac{1}{2}\sqrt{\frac{\hbar\omega^3}{m_1 g}}(1 + \frac{\Delta m}{m_1})^{-\frac{1}{2}} \tag{3.26}$$

$$\lambda_c^{(2)} = \frac{\sqrt{\kappa_1}}{2}(1 - \frac{\Delta m}{2m_1}) \tag{3.27}$$

We may express $\lambda_c^{(2)}$ as

$$\lambda_c^{(2)} \approx \lambda_c^{(1)} - \Delta\lambda \tag{3.28}$$

where $\Delta\lambda \equiv \frac{\Delta m}{2m}\lambda_c^{(1)}$.

Hence, if we chose set of experimental parameters such that modulation strength λ is smaller than$\lambda_c^{(1)}$ but greater than $\lambda_c^{(2)}$, atoms of the isotope of mass m_1 will stay localized, whereas the atoms of the other isotope of mass m_2

will show classical diffusion and spread above the modulated atomic mirror, as shown in Fig.We know the location of the localized isotope, therefore, by using an intense laser we can extract them and store in a chamber.

3.6.1 An analysis

An atomic wave packet,displays an exponential localization behavior both in the momentum space and position space,when propagated in the Fermi accelerator. Furthermore,it occurs for a time beyond quantum break time, and for a modulation strength within the localization window

$$\lambda_l < \lambda < \lambda_c \tag{3.29}$$

.The final quantum distributions are a manifestation of interference phenomena, thereby independent of the choice of initial distributions of the wave packet.In the momentum space the atomic wave packet redistributes itself around the initial mean momentum after an evolution over many bounces[59]. For two different isotopes of mass $m1$ and $m2$, two different critical modulation strengths occur, i.e.$\lambda = \lambda_{c1}$ for atoms of mass $m1$ and $\lambda = \lambda_{c2}$ for atoms of mass $m2$.Numerical investigation of the system estimates the quantum mechanical momentum space distribution for the lighter isotope as exponentially localized

$$\Psi(p) \sim e^{-\frac{p}{l}} \tag{3.30}$$

where l describes localization length.

For the heavier isotope the quantum delocalization takes place and momentum distribution obeys the Maxwellian distribution.

$$P_{cl(p)} = (\frac{1}{\sqrt{2\pi E_T}})exp[\frac{-p^2}{2E_T}] \tag{3.31}$$

as in Brownian motion. Here $E_T \equiv \frac{\omega^2 k_B T}{mg^2}$ is the scaled effective thermal energy,k_B and T are Boltzmann's constant and the effective temperature,respectively.

3.7 Numerical results

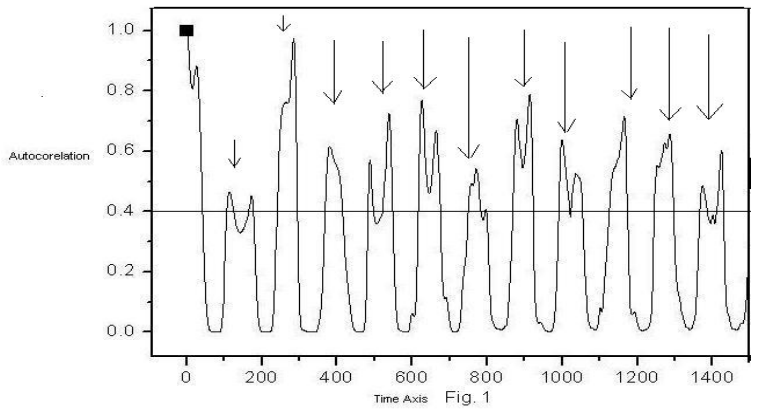

Figure 3.3: Autocorrelation function is plotted against scaled evolution time $\kappa = 4$.

The autocorrelation function is plotted against scaled evolution time. We calculate classical revival time of cold atoms with $\kappa = 4$ .we see in $Figure(3.3)$ reconstruction of Gaussian wave packet at time periodically of the graphs and completely destroyed at other time. In $figure3.4$ the autocorrelation function is plotted against scaled evolution time. We calculate classical revivals time for $\kappa = 1$ with same lamda value. we see that there is no reconstruction of Gaussian wavepacket at all.Which mean that atoms of small mass for which we take $\kappa = 4$ in $figure(3.3)$ are localized while atoms for which we

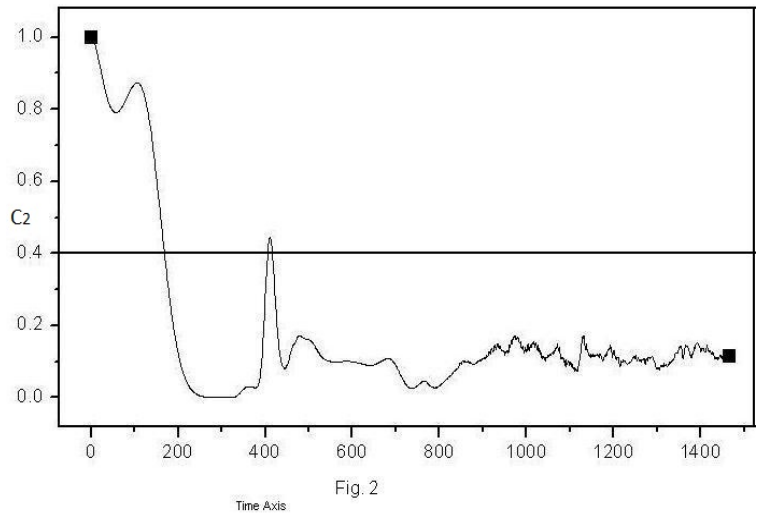

Figure 3.4: Autocorrelation function plotted against scaled evolution time $\kappa = 1$.

take $\kappa = 1$ in $figure(3.4)$ are De-localized.

Infigure3.5 the square of dispersion in momentum (ΔP^2) is plotted against modulation strength(λ) for $\kappa = 3$ to find λ_c for this particular atoms.From this plot we find that $\lambda_c = 0.8$. for these atoms.

In figure(3.6) the square of dispersion in momentumΔP^2 is plotted against modulation strengthλ for $\kappa = 4$ to find λ_c for this particular atoms.From this plot we find that $\lambda_c = 1$. for these atoms.

In figure(3.7) we combine Figure(3.5) and Figure(3.6) to find $\Delta\lambda$.From this plot we see that in $(\lambda - \omega)$ there are three regions:Region I where both of the Isotopes are Localized.Region II where Isotope for which $\kappa = 3$ correspond to large mass is delocalized and Isotope for which $\kappa = 4$ which correspond to small mass are localized.In region III both Isotopes are delocalized.

In figure 3.8 the square of dispersion in momentum (ΔP^2) is plotted against

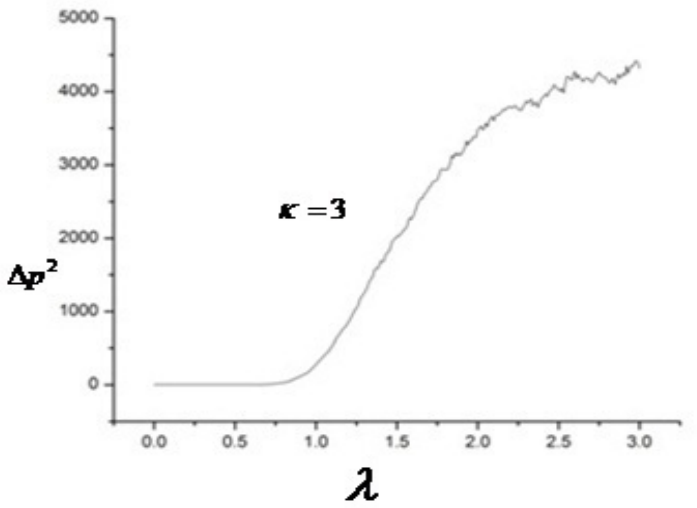

Figure 3.5: The square of dispersion in momentum (ΔP^2) is plotted against modulation strength(λ)

time for inside region.we find the smaller atoms localized and heaver mass delocalized.

In figure(3.9) the square of dispersion in momentum (ΔP^2) is plotted against modulation strength(λ) for Cesium atoms(Cs_{139}) to find λ_c for Cesium(Cs_{139}) atoms.From this plot we find that $\lambda_c = 0.97.$ for Cesium(Cs_{139}) atoms.

In figure(3.10) the square of dispersion in momentum (ΔP^2) is plotted against modulation strength(λ) for Cesium atoms(Cs_{132}) to find λ_c for Cesium(Cs_{132}) atoms.From this plot we find that $\lambda_c = 1.$ for Cesium(Cs_{132}) atoms.

In figure3.11 we combine Figure(3.9) and Figure(3.10) to find $\Delta\lambda$.From this plot we see that in $(\lambda - \omega)$ there are three regions.Region I where both of the Cesium(Cs) Isotopes are Localized.In region II Cs_{139} Isotopes are delocalized and Cs_{132} are localized.In region III both Isotopes are delocalized.As we know location of localization region so by using intense laser beam we can collect Cs_{132} atoms in a chamber.

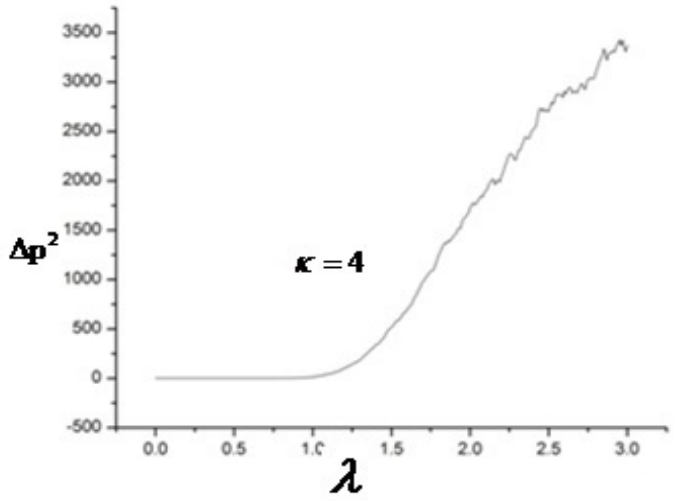

Figure 3.6: The square of dispersion in momentumΔP^2 is plotted against modulation strengthλ for $\kappa = 4$

In figure(3.12) the square of dispersion in momentum (ΔP^2) is plotted against modulation strength(λ) for Hydrogen atoms(H_3)($Tritium$) to find λ_c for Hydrogen(H_3) atoms.From this plot we find that $\lambda_c = 13.2.$ for Hydrogen(H_3) atoms.

In figure(3.13) the square of dispersion in momentum (ΔP^2) is plotted against modulation strength(λ) for Hydrogen atoms(H_2)($Deuterium$) to find λ_c for Hydrogen(H_2) atoms.From this plot we find that $\lambda_c = 16.2.$ for Hydrogen(H_2) atoms.

In figure3.14 we combine Figure(3.12) and Figure(3.13) to find $\Delta\lambda$.From this plot we see that in $(\lambda - \omega)$ there are three regions.Region I where both of the Cesium(Cs) Isotopes are Localized.In region II H_3 Isotopes are delocalized and H_2 are localized.In region III both Isotopes are delocalized.As we know location of localization region so by using intense laser beam we can collect H_2 atoms in a chamber.

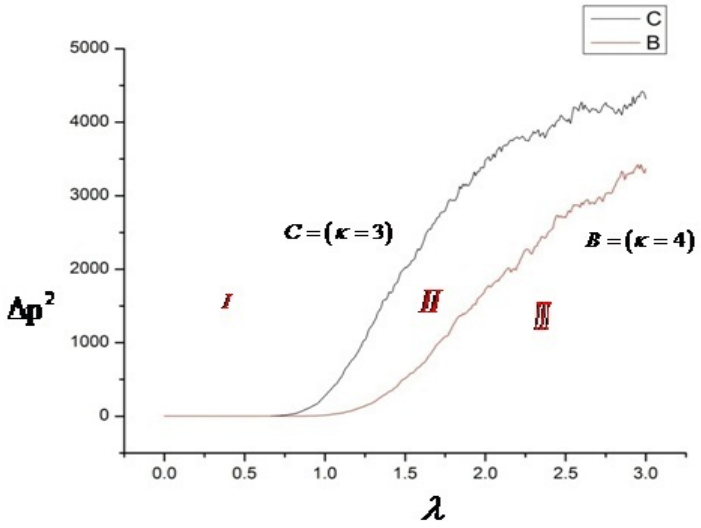

Figure 3.7: This plot shows that in $(\lambda - \omega)$ space there are three regions:Region I where both of the Isotopes are Localized.Region II where Isotope for which $\kappa = 3$ correspond to large mass is delocalized and Isotope for which $\kappa = 4$ which correspond to small mass are localized.In region III both Isotopes are delocalized.

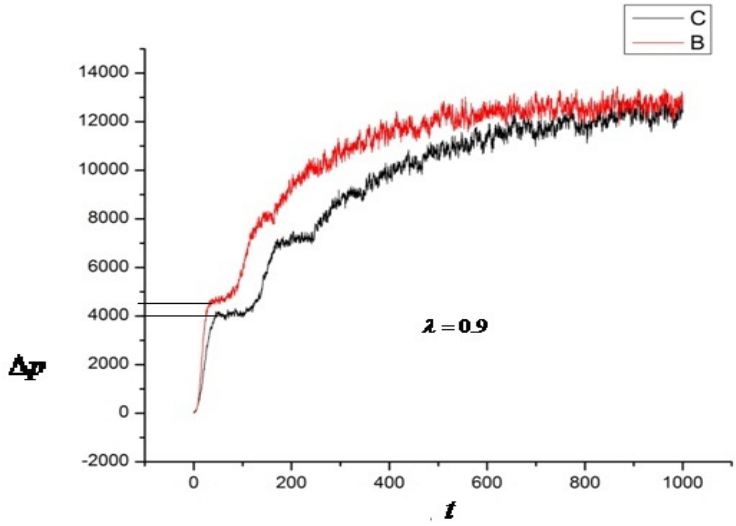

Figure 3.8: The square of dispersion in momentum (ΔP^2) is plotted against time for inside region.we find the smaller atoms localized and heaver mass delocalized.

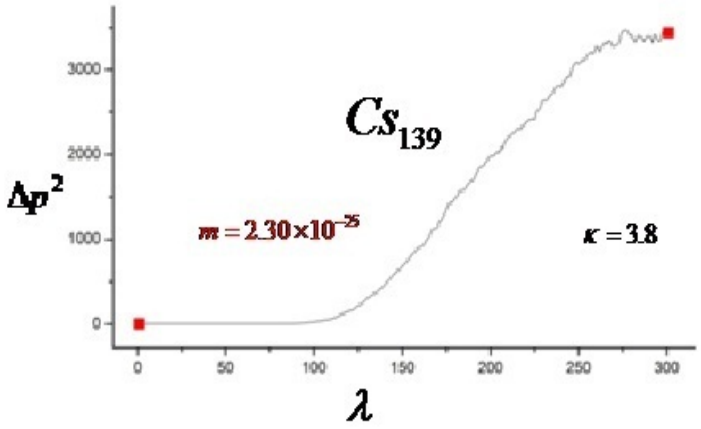

Figure 3.9: The square of dispersion in momentum (ΔP^2) is plotted against modulation strength(λ) for Cesium atoms(Cs_{139})

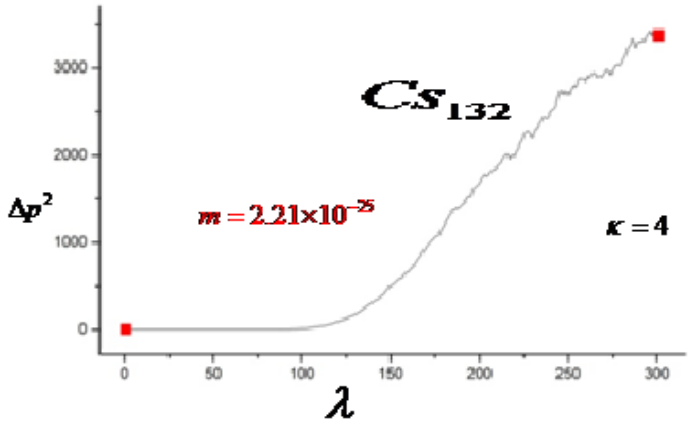

Figure 3.10: The square of dispersion in momentum (ΔP^2) is plotted against modulation strength(λ) for Cesium atoms(Cs_{132})

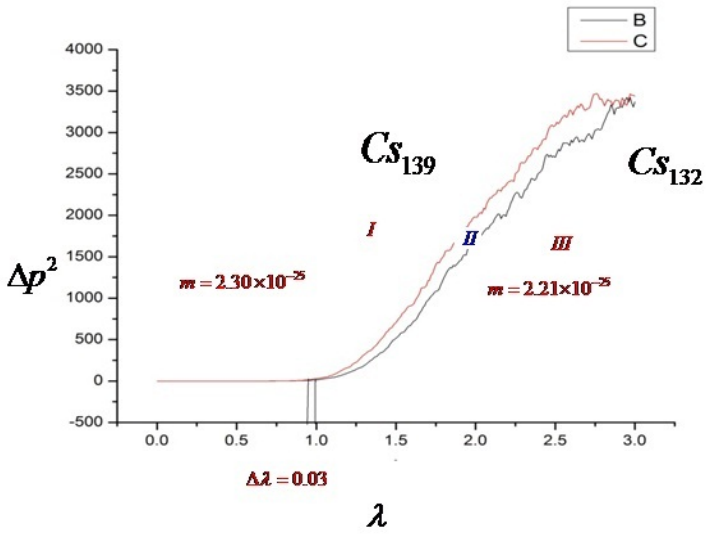

Figure 3.11: This plot shows that in $(\lambda - \omega)$ there are three regions.Region I where both of the Cesium(Cs) Isotopes are Localized.In region II Cs_{139} Isotope is delocalized and Cs_{132} are localized.In region III both Isotopes are delocalized.As we know location of localization region so by using intense laser beam we can collect Cs_{132} atoms in a chamber.

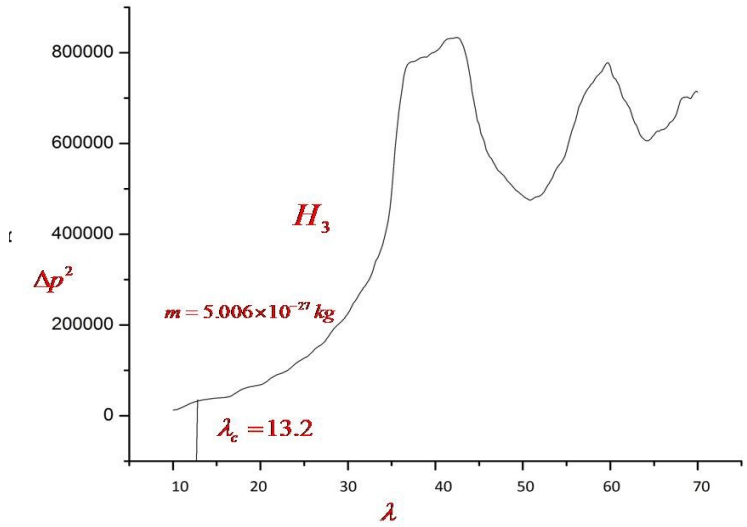

Figure 3.12: The square of dispersion in momentum (ΔP^2) is plotted against modulation strength(λ) for Hydrogen atoms(H_3)($Tritium$)

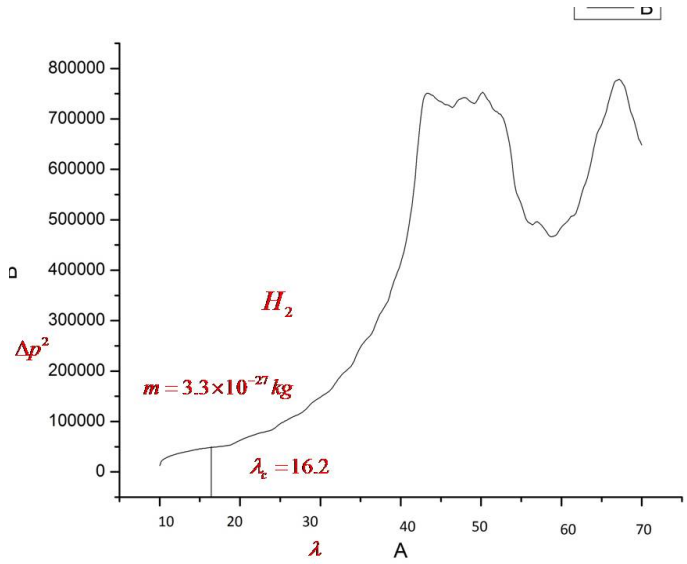

Figure 3.13: The square of dispersion in momentum (ΔP^2) is plotted against modulation strength(λ) for Hydrogen atoms(H_2)($Deuterium$)

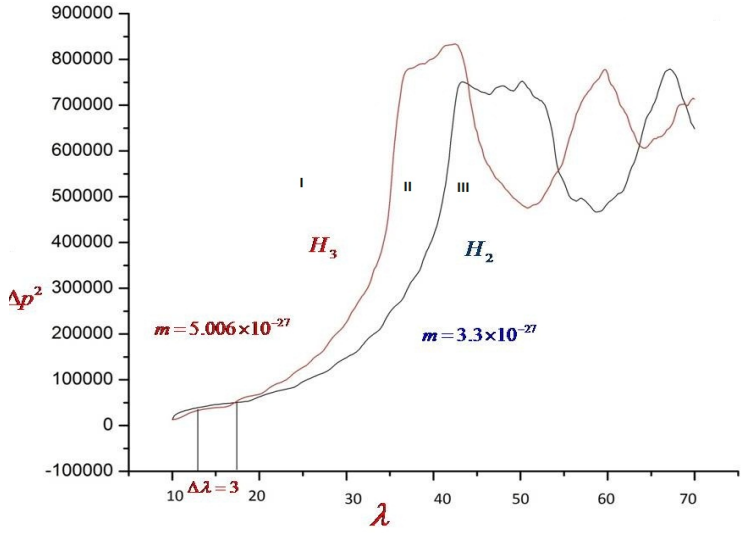

Figure 3.14: This plot shows that in $(\lambda - \omega)$ there are three regions.Region I where both of the Hydrogen(H) Isotopes are Localized.In region II H_3 Isotope is delocalized and H_2 are localized.In region III both Isotopes are delocalized.As we know location of localization region so by using intense laser beam we can collect H_2 atoms in a chamber.

Chapter 4

Conclusions

A new method for the separation of isotopes was proposed by Dr. F. Saif. This method is based on dynamical de-localization of the atomic wave packets. It is proposed for the separation of ultra cold atoms. The present work is based on numerically exploring the possibility of its use as real separation method. In the first part of the work the method was numerically evaluated. An important part of the assembly for the proposed separator machine is mirror. There are two major mirrors used to bounce ultra cold atoms which are blue detuned evanescent mirrors and magnetic mirrors. Magnetic mirrors are used for trapping and storing while evanescent mirrors are mainly used for bouncing back. As our system need potential well, we used a blue detuned evanescent acusto optic wave mirror placed normal to the gravitational field. Other components of the proposed separator include laser source, acusto optic modulator, the laser field, the separation system and the collector. All these are thoroughly discussed and numerically treated. It was concluded that by the use of an appropriate assembly this method is feasible for the effective separation of isotopes. We discuss Localization window and explain its lower and upper limits. We also discuss localization of atoms inside local-

ization window. We calculate dependence of modulation strength on mass of isotopes and external frequency and also find equation for region which tell us about the position of localized atoms. We find different critical modulation strength for different Isotopes of Hydrogen and Cesium atoms and also find localization window for these Isotopes. The technique proposed here can be applied to different materials. As an important advantage of the technique is that we know the delta-lambda region numerically, hence by using an intense laser we can extract one isotope. This approach is different from Laser isotope separation because in laser isotope separation finely tuned laser beam is used for ionization of particular atoms while in our case we use radiation pressure.

Bibliography

[1] F. A. Cotton, G. Wlikinson and P. L. Gaus. Basic Inorganic Chemistry,Third edition. John Willy and Sons 2001.

[2] B. Moody. Comparative Inorganic Chemistry,Third edition Edward Arnold 1991.

[3] G. C. Hill and J. S. Holman. Chemistry in Context,Third edition John Willy and Sons 2001.

[4] Robert W.Parry, Herb Bassow and Phyllis Merrill.Chemistry Experimental Foundation, Fourth edition Prentice-Hall.

[5] From Wikipedia.

[6] Gea-Banacloche, J., 1999. Am. J. Phys. 67, 776.

[7] Bordo, V.G., Henkel, C., Lindinger, A., Rubahn, H.G., 1997. Opt. Commun. 137, 249.

[8] Mandel, L., 1986. Phys. Scr. T 12, 34-42. Mandel, L., Wolf, E., 1995. Optical Coherent and Quantum Optics. Cambridge University Press.

[9] Jackson, J.D., 1965. Classical Electrodynamics. Wiley, New York.

[10] Balykin, V.I., Letokhov, V.S., 1989. Appl. Phys. B 48, 517.V.I., Letokhov, V.S.,Ovchinnikov, Y.B., Sidorov, A.I., 1987. Pis'ma Zh. Eksp. Teor. Fiz. 45, 282 [JETP Lett. 45 (1987) 353].

[11] Aminoff, C.G., Steane, A.M., Bouyer, P., Desbiolles, P., Dalibard, J., Cohen-Tannoudji, C., 1993. Phys. Rev. Lett. 71, 3083.

[12] Henkel, C., MZlmer, K., Kaiser, R., Vansteenkiste, N., Westbrook, C., Aspect, A., 1997. Phys. Rev. A 55, 1160.

[13] V. S.Letokhov,V. G.Minogin, and Pavlik,B. D. Opt. Comm. **19**, 72, (1976).

[14] Chu, S. Bjorkholm, J. E. Ashkin, A. and Cable, A. Phys. Rev. Lett. **57**,314, (1986).

[15] Miller, J. D., Cline, R. A., Heinzen, D. J. Phys. Rev. A **47**, R4567, (1994).

[16] Adams, C. S., Lee, H. J., Davidson, N., Kasevich, M., and Chu, S. Phys. Rev. Lett. **74**, 3577, (1995).

[17] K. L. Corwin, S. J. M. Kuppens, D. Cho, and C. E. Wieman, Phys. Rev. Lett. **83**, 1311, (1999).

[18] Kuga, T. Torii, Y., Shiokawa, N., Hirano, T., Shimizu, Y., and Sasada, H. Phys. Rev. Lett. **78**, 4713, (1997).

[19] Ozeri, R., Knaykovich, L., and Davidson, N., Phys. Rev. A **59**, R1750, (1999).

[20] Takekoshi, T., and Knize, R. J., Opt. Lett. **21**, 77, (1996).

[21] O'Hara, K. M., Granado, S. R., Gehm, M. E., Savard, T. A., Bali, I., Freed, C. fig and Thomas, J. E., Phys. Rev. Lett. **82**, 4204, (1999).

[22] Balykin, V. I., Letokhov, V. S., Ovchinnikov, Yu. B., Sidorov, A. I., and Shulga, S. V., Opt. Lett. **13**, 958, (1988b).

[23] Balykin, V. I., Lozovik, Yu. E., Ovchinnikov, Yu. B., Sidorov, A. I., Shulga, S. V., and Letokhov, V. S. J. Opt. Soc. Am. B **6**, 2178, (1989).

[24] Ovchinnikov, Yu. B., and Letokhov, V. S. Comm. At. Mol. Phys, **27**, 185, (1992).

[25] Westbrook, C. I., Watts, R. N., Tanner, C. E., Rolston, S. L., Phillips, W. D., Lett, P. D., and Gould, P. L. Phys. Rev. Lett. **65**, 33, (1990).

[26] Jessen, P. S., Gerz, C., Lett, P. D., Phillips, W. D., Rolston, S. L., Spreeuw, R. J. C., and Wesrbrook, C. I. Phys. Rev. Lett. **69**, 49, (1992).

[27] Guidoni, L., Triche, C., Verkerk, P., and Grynberg, G. Phys. Rev. Lett. **79**, 3363, (1997).

[28] Grynberg, G., Lounis, B., Verkerk, P., Courtois, J.-Y., and Salomon, C. (1997). Phys. Rev. Lett. **70**, 2249, (1997).

[29] Petsas, K. I., Coates, A. B., and Grynberg, G. Phys. Rev. A **50**, 5173, (1994).

[30] Jessen, P. S., and Deutsch, I. H. Adv. Atom. Mol. Opt. Phys. **37**, 95, (1996).

[31] Ovchinnikov, Yu. B., Shul'ga, S. V., and Balykin, V. I. J. Phys. B **24**, 3173, (1991).

[32] Ovchinnikov, Yu. B., Shul'ga, S. V., and Balykin, V. I. J. Phys. B 24, 3173.(1991).

[33] Desbiolles, P., and Dalibard, J. Opt. Comm. **132**, 540, (1991).

[34] Power, W. L., Pfan, T., and Wilkins, M. Opt. Comm. **143**, 25, (1997).

[35] Hinds, E. A., Boshier, M. G., and Hughes, I. G. Phys. Rev. Lett. **80**, 645, (1998).

[36] Ol'shanii, M. A., Ovchinnikov, Yu. B., and Letokhov, V. S. Opt. Comm. **98**, 77, (1993).

[37] Solimeno, S., Grosignani, B. B., and Diponto, P. Guiding, *Diffraction, and Confinement of Optical Radiation*, (Academic Press, New York, 1986).

[38] Renn, M. J., Montgomery, D., Vdovin, O., Anderson, D. Z., Wieman, C. E., and Cornell, E. A. Phys. Rev. Lett. **75**, 3253, (1995).

[39] Savage, C. M., Marksteiner, S., and Zoller, P. *Fundamentals of Quantum Optics III*, (Ed. F. Ehlotzky. Springer, Berlin, 1993).

[40] Marksteiner, S., Savage, C. M., Zoller, P., and Rolston, S. L. Phys. Rev. A **50**, 2680, (1994).

[41] Ito, H., Nakata, T., Sakaki, K., Ohtsu., M., Lee, K. I., and Jhe, W. Phys. Rev. Lett. **76**, 4500, (1996).

[42] Pillof, H. C. Opt. Comm. **143**, 25, (1997).

[43] Balykin, V.I. Adv. At. Mol. Opt. Phys. **41**, 181, (1999).

[44] Fam Le Kien, V. I. Balykin,and K.Hankuta Phys. Rev. A **70**, 063403, (2004).

[45] Svelto, O., Hanna, D.C., 1998. Principles of Lasers. fourth ed. Plenum, New York, NY.

[46] Matsudo , (1997).

[47] Kasevich, M.A., Weiss, D.S., Chu, S., 1990. Opt. Lett. 15, 607. Wallis, H., Dalibard, J., Cohen-Tannoudji, C., 1992. Appl. Phys. B 54, 407.

[48] Anderson, P.W., 1958. Phys. Rev. 109, 1492.

[49] Anderson, P.W., 1959. Phys. Rev. 115, 2.

[50] Casati, G., Chirikov, B.V., Ford, J., Izrailev, F.M., 1979. Lecture Notes Phys. 93, 334.

[51] Fishman, S., Grempel, D.R., Prange, R.E., 1982. Phys. Rev. Lett. 49, 509.

[52] Haake, F., 1992. Quantum Signatures of Chaos. Springer, Berlin. Altland, A., Zirnbauer, M.R., 1996. Phys. Rev. Lett. 77, 4536. Zaslavsky, G., 1981. Phys. Rep. 80, 157.

[53] Brody, T.A., Flores, J., French, J.B., Mello, A., Pandy, A., Wong, S.S.M., 1981. Rev. Mod. Phys. 53, 385.Bohigas, O., Giannoni, M.J., Schmit, C., 1984. Phys. Rev. Lett. 52, 1.

[54] Jose, J.V., Cordery, R., 1986. Phys. Rev. Lett. 56, 290.

[55] Jose, J.V., 1991. In: Cerdeira, H.A., Ramaswamy, R., Gutzwiller, M.C., Casati, G. (Eds.), Quantum Chaos. Proceedings of the Adriatico Research Conference and Miniworkshop, Trieste, Italy, 4 June-6 July 1990.

World Scientific, Singapore. Dana, I., Eisenberg, E., Shnerb, N., 1995. Phys. Rev. Lett. 74, 686. Prange, R.E., 1991. In: Cerdeira, H.A., Ramaswamy, R., Gutzwiller, M.C., Casati, G. (Eds.), Quantum Chaos. Proceedings of the Adriatico Research Conference and Miniworkshop, Trieste, Italy, 4 June-6 July 1990. World Scientific, Singapore.

[56] Oliveira, C.R.de., Guarneri, I., Casati, G., 1994. Europhys. Lett. 27, 187. Benvenuto, F., Casati, G., Guarneri, I., Shepelyansky, D.L., 1991. Z. Phys. B 84, 159.

[57] Chirikov,B.V.,1979. Phys. Rep. 52, 263.

[58] Saif F 2000 Phy. Lett. A 274 98 Saif F 2005 Phys.

[59] Saif F 2006 Phys.Rep.425 369